Vibration Transmissibility as a Method of Damage Detection on Horizontal Axis Wind Turbine Blades

RACHEL HENDERSON, ANTHONY SINCLAIR and FAE AZHARI

ABSTRACT

Structural health monitoring of horizontal axis wind turbine blades is challenging due to their large size and limited in-service accessibility. Given the harsh environment that wind turbines operate in, the blades are prone to damage throughout their working life. This paper examines the transmissibility of vibration response among embedded sensors over time as a method of damage characterization. After damage occurs, the sensors closest to the new defect will experience the highest change in transmissibility compared to baseline readings. The defect can therefore be identified and located with this method. When assessed at the natural frequencies of the blade, the response transmissibility between two sensors is independent of applied force and magnitude. This makes vibration transmissibility an ideal method for inspecting wind turbine blades that are subject to varying wind speed and direction.

A blade was designed based on the NREL IEA Wind -15MW offshore reference wind turbine, with modifications made to fabricate a scaled 3D printed model for testing. The blade was outfitted with MEMs accelerometers to measure acceleration and fiber Bragg gratings (FBGs) to measure strain. To test the transmissibility concept prior to experimental testing, a finite element model was developed to simulate acceleration and strain transmissibility on a damaged and undamaged blade with random force inputs. This model was able to demonstrate that a 5mm transverse crack was visible across the blade when examined at the natural frequencies.

INTRODUCTION

Wind turbine blades are prone to defects and failure given their difficult operating environment. In-service inspections of wind turbine blades are primarily conducted with visual techniques [1]. Visual inspection utilizes rope-access technicians, cameras or drones to fully assess the blade condition. This type of inspection, although effective, only provides an overview of the condition at intermittent points in time. There is a need

Department of Mechanical & Industrial Engineering, University of Toronto, 5 King's College Road, Toronto, ON M5S 3G8, Canada

for continuous monitoring of the blades to identify defects as early as possible and prevent major damage and catastrophic blade failure.

Vibration monitoring is often used on the drive train, blades and the towers to ensure the wind turbine remains within its safe operating window [2]. It is also used for damage detection, primarily on the drive train. For large structures such as the blade, it is difficult to assess the condition with vibration analysis as changes to the vibration signature are often minimal unless the damage is severe. This paper examines the feasibility of vibration transmissibility, a subset of vibration analysis, as a method of continuous structural health monitoring of the blades.

TRANSMISSIBILITY THEORY

Transmissibility examines outputs of different sensor pairs in an array. This concept has been covered extensively in [3], [4], [5] and [6]. To explain the theory, consider the two locations i and j on the wind turbine blade in Figure 1 when exposed to force $F(\omega)$ at location k. The equation for the transmissibility between i and j can be found in Equation 1 below, where $X(\omega)$ is the output response and $H(\omega)$ is the frequency response function (FRF).

$$T_{ijk}(\omega) = \frac{X_{ik}(\omega)}{X_{jk}(\omega)} = \frac{H_{ik}(\omega)F_k(\omega)}{H_{jk}(\omega)F_k(\omega)} \tag{1}$$

The FRFs, $H_{ik}(\omega)$ and $H_{jk}(\omega)$, are dependent on the mass, damping and stiffness of the material. These functions will be affected by the occurrence of damage and will therefore cause a change in the transmissibility T_{ijk} when compared to a baseline value.

In Equation 1, the force function $F_k(\omega)$ cancels out and the transmissibility becomes a ratio of the output responses $X_{ik}(\omega)$ and $X_{jk}(\omega)$ if the location k of the force is known. The wind force location is constantly changing for a wind turbine blade in service, so further information on the forces would be required to utilize the transmissibility method in this format.

The transmissibilities and the FRFs were measured across the frequency range with different force locations in [7]. This research found that at the natural frequencies, the transmissibilities converge to a common value. Therefore, Equation 1 can be rewritten at the natural frequency ω_n, as:

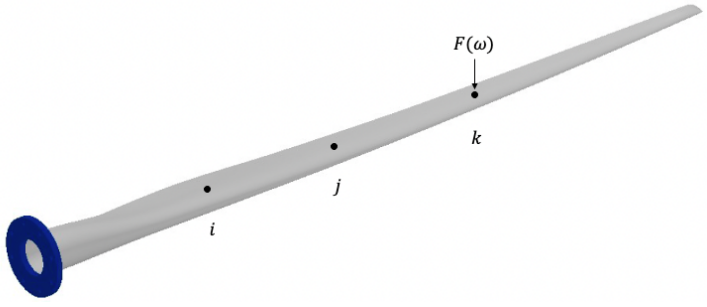

Figure 1. Wind turbine blade layout with sensor locations i and j and input force at k.

$$T_{ij}(\omega_n) = \frac{X_i(\omega_n)}{X_j(\omega_n)} = \frac{H_i(\omega_n)F_k(\omega_n)}{H_j(\omega_n)F_k(\omega_n)} = \frac{H_i(\omega_n)}{H_j(\omega_n)} \quad (2)$$

In Equation 2, the force magnitude and location cancel out, and the transmissibility is completely independent of the applied force. As a result, a wind turbine blade can be monitored under any wind conditions if the transmissibility analysis is conducted at the blade's natural frequencies.

The equation used to calculate the change in transmissibility can be found in Equation 3 [8].

$$D_{ij} = \frac{T_{ij_{Damaged}}(\omega_n) - T_{ij_{Undamaged}}(\omega_n)}{T_{ij_{Undamaged}}(\omega_n)} \quad (3)$$

In this paper, the change in transmissibility is examined across all possible pairs of sensors at the natural frequencies when the blade is exposed to damage. The Total Method sums sensor pairs with a common numerator to give an overall value for the numerator sensor. The equation for the Total Method can be found in Equation 4.

$$Y_i(\omega_n) = \sum D_{ij}(\omega_n) + D_{ij+1}(\omega_n) + \cdots D_{ij+n}(\omega_n) \quad (4)$$

Comparing the results for each sensor $\boldsymbol{Y_i}$ can yield information that damage has occurred as well as provide an approximate location for the defect when comparing all sensors in the array.

EXPERIMENTAL SET-UP

A wind turbine blade was designed based on the NREL IEA Wind -15MW offshore reference wind turbine [9]. The NREL design was scaled to 1.17 meters and minor changes were made to the airfoils, chord width and blade thickness to make it suitable for 3D printing. The blade was printed in sections using the fused filament fabrication (FFF) method and Raise3D Premium PLA. The segments were then glued together and attached to a flange for mounting to an optical table for evaluation.

Two types of sensors were selected for testing. A set-up using MEMs MPU6050 accelerometers were placed on the upper side of the blade. Due to limitations in sampling rate of the Arduino microcontroller, only 8 accelerometers were implemented. These sensors were placed every 10cm from 10cm to 80cm along the length of the blade. A 12-sensor set-up using fiber Bragg gratings (FBGs) was added to the lower side of the blade to measure strain. Eleven of these sensors were located at 10cm intervals from 10cm to 110 cm along the blade. An additional FBG sensor was located next to the blade to compensate for temperature changes during the tests. A diagram of the sensor layout can be seen in Figure 2.

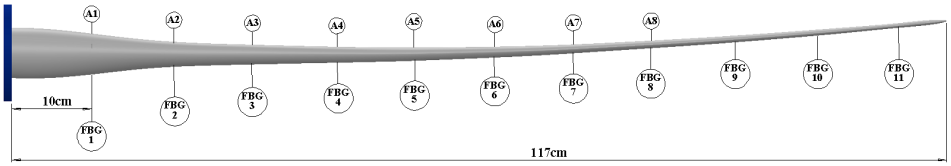

Figure 2. Accelerometer and fiber Bragg grating layout on the wind turbine blade

FINITE ELEMENT SIMULATION

Material

The finite element solver ANSYS was used to simulate the 3D printed blade. Material characterization tests were performed to determine the mechanical properties for the 3D printed material. Raise3D Premium PLA coupons were printed and glued using the same parameters as the wind turbine blade pieces. The coupons were then measured, weighed, and tested under uniaxial tension to determine the Young's modulus. Results from this testing can be found in Table I below. Poisson's ratio was estimated to be 0.33 based on experimental results in [10]. The PLA material was also assumed to be isotropic for the numerical model.

Method

A Solidworks model of the 3D printed blade design was used for the ANSYS simulation. The attachment flange was also included and modeled as a fixed support. This design had 7mm boxes drawn on the surface of the blade at 50% chord span to represent the sensors. Distributed masses were added at these locations to reflect the added weight from the sensors and their auxiliary equipment.

A force was created for each model in the ANSYS harmonic response module. Each force had an X, Y and Z component with arbitrary magnitudes. A random location was selected for each applied force. In addition, a value of 1.2% was selected for the damping ratio. This is based off an average of the results in [11], which characterizes the damping ratios of 3D printed PLA with different printing parameters.

The harmonic response was calculated at frequency intervals of 0.05 Hz from 0 to 50 Hz. Frequency response results for the X, Y and Z directions were determined for both normal strain and acceleration at each sensor location. The X, Y and Z orientations can be viewed in Figure 3. The results were then analyzed using Python code to calculate changes in the transmissibilities at the natural frequencies.

Damage

The initial damage type selected for testing was a transverse through-wall crack of approximate dimensions of 5mm × 1mm. This defect was located on the leading edge of the blade. Eleven damage models were assessed in total with each crack placed at 10cm intervals to determine whether the crack location could be identified. An example of the damage used in the simulations can be found in Figure 3.

TABLE I. 3D PRINTED PLA MATERIAL PROPERTIES - ANSYS

Density (kg/m3)	Young's Modulus (MPa)	Poisson's Ratio
1128	2984	0.33 [10]

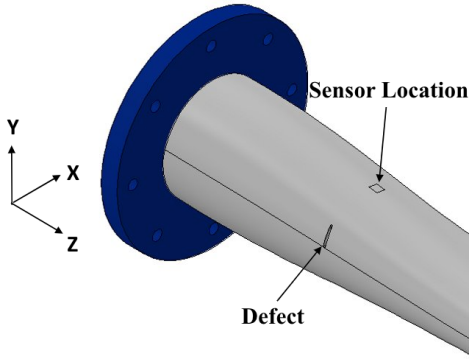

Figure 3. A transverse crack (5mm long and 1mm wide) located at 10cm from the blade hub.

RESULTS

Preliminary results have been collected using the ANSYS numerical model. Using Equations 3 and 4, the real, imaginary, amplitude and phase transmissibilities for each damaged blade were compared to the undamaged blade. This analysis was completed at the first three natural frequencies in the X, Y and Z directions. The natural frequencies of the undamaged blade can be found in Table II.

Changes in the natural frequencies due to blade damage were minimal for all three modes. The natural frequencies were rounded to the nearest 0.05 Hz to utilize the harmonic response results.

Strain

Analysis of the three modes along the X, Y and Z directions found that the real and phase strain transmissibility comparisons provided no recognizable damage pattern. The imaginary and amplitude comparisons were successful at identifying the damage but were dependent on which mode was being analyzed as well as the direction. Of the three modes examined, Mode 1 had the highest success at identifying the damage location. Figure 4 shows the amplitude and imaginary signal comparisons for the Z direction in Mode 1. In this figure, the 11 damage models are compared. A peak occurs at the sensor where the defect is located for the majority of these models.

TABLE II. ANSYS NATURAL FREQUENCIES OF THE UNDAMAGED BLADE

Mode	Frequency (Hz)
Mode 1 (Flapwise)	9.00
Mode 2 (Edgewise)	22.23
Mode 3 (Flapwise)	27.12

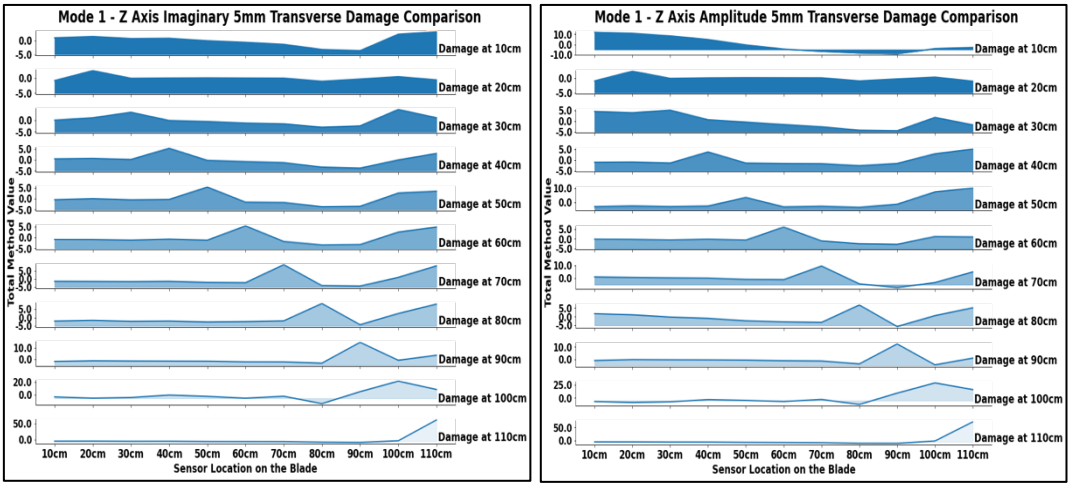

Figure 4. Z direction strain transmissibility results for Mode 1.

Acceleration

Interpretation of the acceleration data was found to be different from the strain data. For acceleration, the Total Method plot intercepts the X axis at the location of the damage. Figure 5 shows this trend with the imaginary and amplitude comparisons for Mode 2 in the X direction. Both plots show X intercepts aligned with the damage location for damage located up to 50cms from the blade hub. Beyond this point, the damage is no longer correctly identified.

Direction in relation to the mode being analyzed was also important when examining the acceleration transmissibilties. The Y direction was the most successful for flapwise modes 1 and 3. The X direction was the most successful for edgewise mode 2. Overall, the second mode in the X direction provided the best damage recognition for the 5mm crack. Similar to the strain data, the real and phase transmissibility comparisons yielded minimal results across all modes.

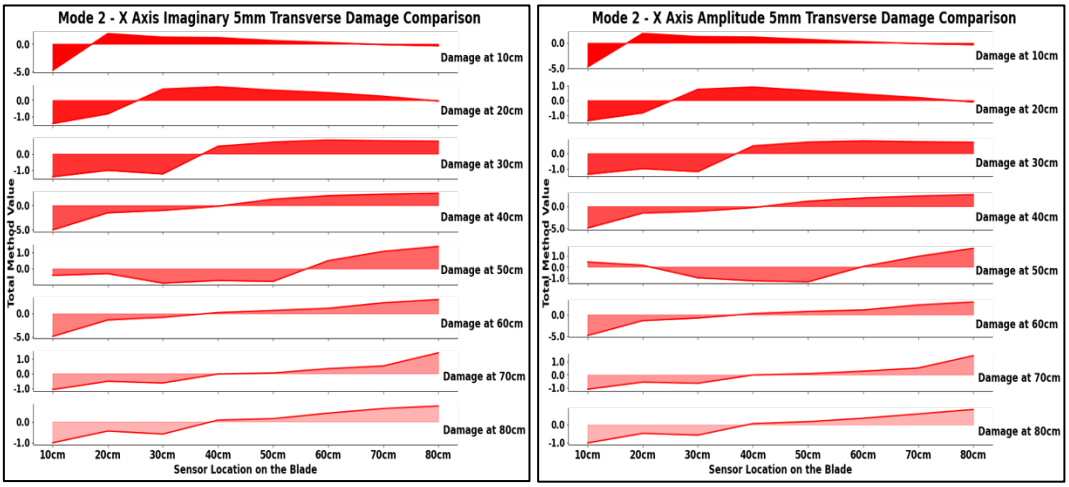

Figure 5. X direction acceleration transmissibility results for Mode 2.

DISCUSSION

One of the challenges of vibration analysis of large structures is the lack of change in the natural frequencies when damage occurs. Comparison of the natural frequencies for the 5mm transverse defect found changes of less than 0.3% across the first 10 modes in the ANSYS simulation. This was regardless of damage location. As a result, traditional vibration analysis would be ineffective for this particular defect. Utilizing the transmissibilities provides a higher sensitivity when it comes to damage detection and can be used to approximate the damage location.

The strain transmissibility was more successful at identifying the 5mm transverse damage. For mode 1, the damage could be identified across most blade locations in at least one direction. Damage was less detectable at smaller distances from the base of the blade. This was in contrast with the acceleration data, where damage closer to the base of the blade was more visible. Sensor orientation and location relative to the defect must be assessed further as strain gauge effectiveness is typically influenced by these factors.

When using the acceleration transmissibility data to examine damage across the full length of the blade, it was noted that the damage was no longer visible beyond 50cm from the blade hub. As many types of wind turbine blade damage occur towards the blade tip, measuring just the acceleration may not be sufficient. Furthermore, defects beyond 60cm yielded results similar to defects at locations of damage closer to the base of the blade. This may lead to false positives.

CONCLUSIONS AND FUTURE WORK

The numerical model results show that it is possible to detect a 5mm × 1mm through-wall transverse crack on a 3D-printed horizontal axis wind turbine blade and identify its approximate location. Strain transmissibility had a higher sensitivity for crack detection than acceleration transmissibility for this damage size and type. It was easier to see that damage had occurred with strain vs the acceleration method and there were fewer limitations on location. The acceleration method was however better at identifying damage closer to the base of the blade. Further numerical analyses and experimental testing is required with other damage types to verify these initial findings.

Full experimental testing is currently in progress to examine the use of fiber Bragg grating strain sensors and MEMs accelerometers to verify the numerical model for the 5mm transverse crack. Future work includes numerical and experimental testing of 5mm x 1mm cracks at different orientations on the leading edge as well as exploring other damage types and locations.

REFERENCES

[1] F. P. García Márquez and A. M. Peco Chacón, “A review of non-destructive testing on wind turbines blades,” *Renew Energy*, vol. 161, pp. 998–1010, Dec. 2020, doi: 10.1016/J.RENENE.2020.07.145.

[2] F. P. García Márquez, A. M. Tobias, J. M. Pinar Pérez, and M. Papaelias, "Condition monitoring of wind turbines: Techniques and methods," *Renew Energy*, vol. 46, pp. 169–178, Oct. 2012, doi: 10.1016/J.RENENE.2012.03.003.

[3] S. Chesné and A. Deraemaeker, "Damage localization using transmissibility functions: A critical review," *Mech Syst Signal Process*, vol. 38, no. 2, pp. 569–584, Jul. 2013, doi: 10.1016/J.YMSSP.2013.01.020.

[4] N. M. M. Maia, J. M. M. Silva, and A. M. R. Ribeiro, "THE TRANSMISSIBILITY CONCEPT IN MULTI-DEGREE-OF-FREEDOM SYSTEMS," *Mech Syst Signal Process*, vol. 15, no. 1, pp. 129–137, Jan. 2001, doi: 10.1006/MSSP.2000.1356.

[5] N. M. M. Maia, A. P. V. Urgueira, and R. A. B. Almei, "Whys and Wherefores of Transmissibility," in *Vibration Analysis and Control - New Trends and Developments*, InTech, 2011. doi: 10.5772/24869.

[6] W. J. Yan, M. Y. Zhao, Q. Sun, and W. X. Ren, "Transmissibility-based system identification for structural health Monitoring: Fundamentals, approaches, and applications," *Mech Syst Signal Process*, vol. 117, pp. 453–482, Feb. 2019, doi: 10.1016/J.YMSSP.2018.06.053.

[7] C. Devriendt and P. Guillaume, "The use of transmissibility measurements in output-only modal analysis," *Mech Syst Signal Process*, vol. 21, no. 7, pp. 2689–2696, Oct. 2007, doi: 10.1016/J.YMSSP.2007.02.008.

[8] H. ZHANG, M. J. SCHULZ, A. NASER, F. FERGUSON, and P. F. PAI, "STRUCTURAL HEALTH MONITORING USING TRANSMITTANCE FUNCTIONS," *Mech Syst Signal Process*, vol. 13, no. 5, pp. 765–787, 1999, doi: https://doi.org/10.1006/mssp.1999.1228.

[9] E. Gaertner *et al.*, "Definition of the IEA 15-Megawatt Offshore Reference Wind," Mar. 2020. Accessed: May 14, 2023. [Online]. Available: https://www.nrel.gov/docs/fy20osti/75698.pdf

[10] R. T. L. Ferreira, I. C. Amatte, T. A. Dutra, and D. Bürger, "Experimental characterization and micrography of 3D printed PLA and PLA reinforced with short carbon fibers," *Compos B Eng*, vol. 124, pp. 88–100, Sep. 2017, doi: 10.1016/J.COMPOSITESB.2017.05.013.

[11] F. Medel, J. Abad, and V. Esteban, "Stiffness and damping behavior of 3D printed specimens," *Polym Test*, vol. 109, p. 107529, May 2022, doi: 10.1016/J.POLYMERTESTING.2022.107529.